A Robust Determination of the Voltage Droop Characteristic of Bipolar Multiterminal-VSC-HVDC-Systems based on the Application of the Particle Swarm Optimization

Michael Endres*, Christoph Hahn*, *Member, IEEE,* Jens Dietrich§, Yannick Fotsing§,
and Matthias Luther*, *Member, IEEE*
*Institute of Electrical Energy Systems
Friedrich-Alexander-University of Erlangen-Nuremberg (FAU), Germany
§Siemens AG, Erlangen

***Abstract*—This paper presents a method for the design of the Voltage Droop Control of a Multiterminal VSC-HVDC system. Implementing a Voltage Droop Control scheme enables the system to withstand faults within the DC system. Two approaches are presented and compared: (I) Droop calculation with respect to electrical limits, and (II) with respect to robustness. Under low power, approach (I) led to insufficient stability. Hence, research into another approach is conducted in order to ensure stability and robustness. To analyse the robustness, a linear model of the Multiterminal system, including AC-network, converter, DC-transmission line and control is developed. In order to ensure stability, other constraints as prevention of power reversal and independence from requiring a specific power distribution were taken into account. Therefore, research was conducted into Particle Swarm Optimization in approach (II). The determination of robustness, based on the gap metric, was used as the objective function. This approach delivers droop constants with optimized robustness and stability as the simulation results show.**

***Index Terms*—DC Voltage Droop Control, Gap Metric, HVDC transmission, Multiterminal VSC-HVDC, Robustness, Particle Swarm Optimization.**

I. Introduction

In the course of the German Energy Transition, more and more wind parks have been built mainly in Northern Germany, whereas more and more solar plants have been built mainly in Southern Germany. During high wind energy infeed and bad photovoltaic conditions, it is necessary to transport the power from the North to the South. This can be done with AC transmission or with High Voltage Direct Current (HVDC). Described in [1], three HVDC links in Germany are planned, where one is a Multiterminal system. For point-to-point connections usually a master-slave controlling concept is used, where one terminal has a voltage-based and the other a power-based controller [2]. This is not applicable for Multiterminal systems, as in case of a fault in the master terminal, the entire system has to be shut down. To overcome this issue, research in the field of the Voltage Droop Control, has been conducted [3]. In this concept, each terminal has both a voltage- and power-controlling behaviour.

For the design process of the Voltage Droop Control, several methods have been analysed. In [4], a continuous local control characteristic is implemented. However, no stability check is conducted. A method with stability check is proposed in [5], where research in the stability of DC Voltage Droop Controllers is carried out. The algorithm proposed in [6] uses the least negative real part of the system eigenvalues in order to find the optimum droop constant. These methods determine the droop constants with no respect to robustness. Therefore this paper analyses and compares two approaches. The first determination is based on electrical limits, whereas the second is based on optimizing the droop constants regarding the robustness. To determine the robustness, an approach using the gap metric is applied. Furthermore, the Particle Swarm Optimization (PSO) is used to solve the optimization problem. All analyses are conducted on an exemplary three terminal bipol HVDC system.

The paper is structured as follows: Section II discusses the Voltage Droop Control and the affection of the control on the power distribution after an outage of a terminal. Section III introduces the multi-input multi-output system derived from a model reduction. Section IV explains the methods determining the Voltage Droop Characteristics and, finally, in Section V the simulation results are presented.

II. Voltage Droop Control

The Voltage Droop Control can be implemented in several ways. A distinction can be drawn between current and power-based control concepts (Fig. 1). Based on an existing control model, in this paper, a power-based Voltage Droop Control is chosen with the DC voltage as the control variable and the DC power as the command variable.

Thus, the Voltage Droop Characteristic reflects the specific behaviour of a voltage change as a function of the DC power (Fig. 2). The steepness of the Droop curve determines the sensitivity of the voltage regarding a power change for a particular station. The slope of the characteristic curve is the inverse of the droop constant K which has the unit $\frac{\mathrm{MW}}{\mathrm{kV}}$.

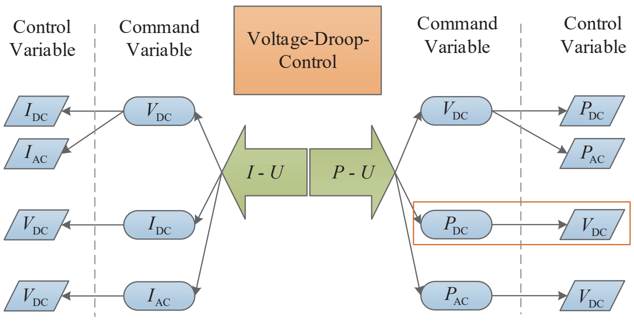

Fig. 1. Overview and classification of the Voltage Droop Control with highlighting of the used approach [5]

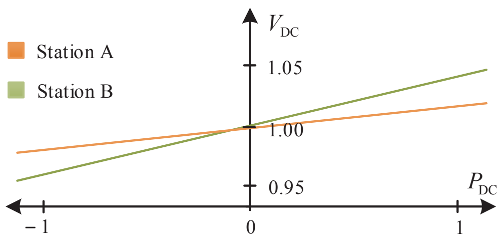

Fig. 2. Example of a Voltage Droop Control characteristic for two stations [7]

For a particular converter station i, a high droop constant K_i or a low slope of the droop curve means that the station balances a large amount of the power imbalance in case of loss of power P_{outage} at another station. The exact amount of power can be quantified with equation (1). The power taken over $\Delta P_{\text{DC},i}$ is indirectly proportional to the droop constant K_i. The deviation of the voltage ΔV_i from the operating set point $V_{SP,i}$ is determined in the following equations:

$$\Delta P_{\text{DC},i} = \Delta P_{\text{outage}} \cdot \frac{K_i}{\sum K_{\text{healthy}}} \tag{1}$$

$$P_{\text{stat},i} = P_i + \Delta P_{\text{DC},i} \tag{2}$$

$$\Delta V_i = \frac{1}{K_i} \cdot \Delta P_{\text{DC},i} \tag{3}$$

$$V_i = V_{\text{SP},i} + \Delta V_i \tag{4}$$

If there is a station in the system which has a very high droop constant compared to the other stations, it can be compared with a voltage-regulating station where the station provides the entire disturbance performance in the event of a fault. If a station has a very low droop constant, it can be regarded as a power controlling station.

The Voltage Droop Characteristic in this work is implemented as a proportional controller as seen in Fig. 3. A change of the set point causes a change of the gain of the controller as well (eq. (13)).

III. Modelling of a MT-HVDC-System

The modelled MTDC-system and its control system which is used for determining the Voltage Droop Control parameters with respect to robustness is shown in Fig. 4. The whole model is divided into an AC and DC part with the respective

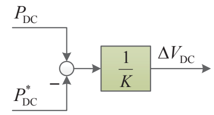

Fig. 3. Block diagram of Voltage Droop Control

controllers. The AC and DC parts are coupled with each other applying an energy model which represents the storage of energy in the sub-module cells of the converters. As shown in the figure, all the quantities are vectors containing six elements each. This is since the whole MTDC system in this work consists of three bipolar HVDC stations, where each station comprises two poles.

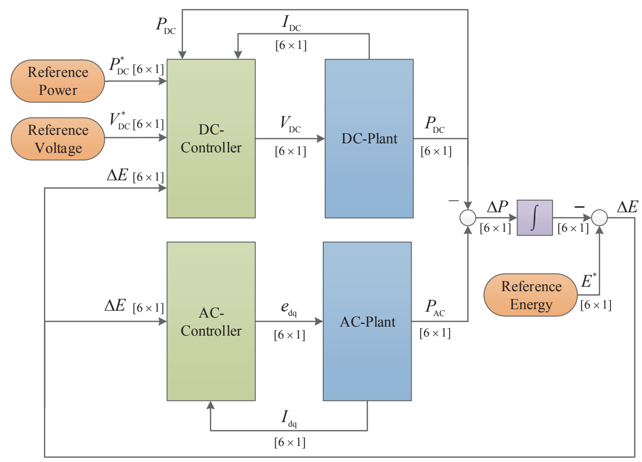

Fig. 4. Block Diagram of the developed MTDC Model with its control

The introduced control structure differs from the well-known control structure applied in conventional VSC-HVDC, as the station control employs a particular control structure with two separate AC and DC control parts. The Voltage Droop Control, designed in the following chapter, is part of the DC controller.

IV. Determination of the Droop Constants

Fig. 5 gives an overview of the two fundamental methods which can be applied to determine the droop constants. In the first approach the determination is conducted with respect to electrical limits, however, without verifying the stability. In the second approach the developed linearised model is evaluated with respect to stability. In this method a droop constant is determined and optimized with regard to robustness. The Particle Swarm Optimization is used as optimization algorithm and afterwards a verification of electrical limits is conducted: E.g., the current is not allowed to exceed a certain limit defined by electrical components.

A. Designing with Emphasis on Electrical Limits

The determination of the Voltage Droop Control characteristic with respect to electrical limits is based on the calculation

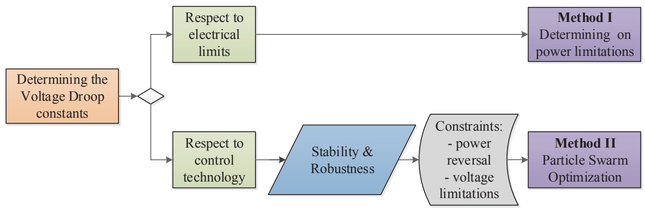

Fig. 5. Methods for the determination of the droop constants with emphasis on robustness

of the sum of the droop constants, which are afterwards distributed to each station. It is assumed that the voltage drop across the DC-impedances is neglected.

Substituting equation (3) in equation (1) and specifying a permissible voltage range $\Delta V_{\max}$ as well as a permissible outage power ΔP_{All} (eq. (5)) delivers the sum of the droop constants. The permissible voltage range is defined by voltage limitations of the system. The permissible outage power follows from the change of the power of a station from its positive to negative power limitation.

$$\sum K = \frac{\Delta P_{\mathrm{All}}}{\Delta V_{\max}} \tag{5}$$

$$\Delta P_{\mathrm{All}} = 2 \cdot \sum_{i=1}^{k} |P_{\max,i}| \tag{6}$$

with k: Number of poles of the system

Afterwards, the distribution of the droop constants is conducted according to eq. (7). Each station is able to participate in case of a fault within the range starting at the current operating point to its positive or negative power limitation, see eq. (8).

$$K_i = \frac{\Delta P_{\mathrm{Lim},i}}{\sum_{i=1}^{k} \Delta P_{\mathrm{Lim}}} \cdot \sum K \tag{7}$$

$$\Delta P_{\mathrm{Lim},i} = |P_{\mathrm{SP},i}| + |P_{\max,i}| \tag{8}$$

$i \in \{\mathrm{A_p}, \mathrm{A_n}, \mathrm{B_p}, \mathrm{B_n}, \mathrm{C_p}, \mathrm{C_n}\}$:

Pol p, n of station A, B oder C

The aim of the Voltage Droop Control concept of this work is to balance power imbalances after the tripping of a station. Whereas changes of the setpoints are performed by the grid controller by changing power and voltage set points very slow. Consequently, the maximal power change is not twice the sum of the power limitation (eq. (6)), but the highest absolute value of the power of the stations (eq. (9)).

$$\Delta P_{\mathrm{All}} = |\Delta P_{\mathrm{Outage,max}}| = \max(|P_{\mathrm{A}}|, |P_{\mathrm{B}}|, |P_{\mathrm{C}}|) \tag{9}$$

In this concept a power imbalance can only occur after an outage of a station and not from a change of set points. As power imbalance is only distributed over the healthy stations (eq. (1) - eq. (4)), it is possible that the voltage range can be exceeded. To overcome this issue, the sum of the droop constants is multiplied by 2. In a worst case scenario, the droop constant of the tripped station is $0.5 \cdot \sum K$. In this case, the other 50 % of the sum droop constant is distributed over the two healthy stations and the stations react on the power imbalance with a voltage change. As the imbalance is split up over two instead of three stations, the sum of the droop constants is distributed over three stations and therefore the maximum voltage range exceeds up to 100 %. By multiplying the sum of the droop constants with 2, this issue can be solved. A droop constant higher than $0.5 \cdot \sum K$ can not be achieved by applying this method, since in stationary state a power equilibrium must occur. Consequently, the sum of the droop constants can be determined as follows:

$$\sum K = 2 \cdot \frac{\Delta P_{\mathrm{Outage,max}}}{\Delta V_{\max}} \tag{10}$$

As power reversal is not permitted, the maximum available power for each station $\Delta P_{\mathrm{Lim},i}$ is equal to its power in the set point $P_{\mathrm{SP},i}$. Thus, the distribution of the droop constants in eq. (7) must be adapted.

$$K_i = \frac{|P_{\mathrm{SP},i}|}{\sum_{i=1}^{k} \Delta P_{\mathrm{Lim}}} \cdot \sum K \tag{11}$$

The sum of the power limitations follows from the power balance:

$$\sum \Delta P_{\mathrm{Lim}} = 2 \cdot P_{\mathrm{Outage,max}} \tag{12}$$

Substituting eq. (10) in eq. (11) results in the simplified calculation of the droop constants.

$$K_i = \frac{|P_{\mathrm{SP},i}|}{\Delta V_{\max}} \tag{13}$$

Consequently, the droop constant is proportional to the absolute value of the power set point and independent from the power set points of the other stations.

B. Designing with Emphasis on Robustness

As seen before, applying a determination with respect to electrical limits doesn't comprise a stability check and the system might be unstable. By using the developed MIMO system of chapter III, it is possible to verify and optimize the stability [8]. Nevertheless, a linear plant model is affected with uncertainties and can describe the system only in an approximated behaviour. Thus, a determination with respect to robustness is strived. A robust controlling method aims to achieve robust performance and stability in the presence of bounded modelling errors or uncertainties. Consequently, a controller is developed in the following to stabilize not only the modelled plant but a sum of the plant $G_{\mathrm{s}}(\mathrm{s})$ and uncertainties $\Delta M(\mathrm{s})$.

$$G(\mathrm{s}) = G_{\mathrm{s}}(\mathrm{s}) + \Delta M(\mathrm{s}) \tag{14}$$

To determine the robustness, an approach of [9] is applied. It derives the normalized co-prime stability margin R from equation (15), where P is the transfer function of the plant, C is the transfer function of the controller and I is the identity matrix.

$$R = \left\| \begin{bmatrix} I \\ C \end{bmatrix} (I - PC)^{-1} \begin{bmatrix} P & I \end{bmatrix} \right\|_{\infty}^{-1} \tag{15}$$

This approach is based on the gap metric between the modelled system and a system afflicted with uncertainties, described in [10]. The higher the uncertainties are allowed to be, the higher is the robustness of the system and consequently of the controller. The determined value is a measurement for the robustness and is maximized by the optimization process. The higher the robustness margin is, the less susceptible to perturbations is the system. If the system is unstable, the robustness margin is 0. This functionality is implemented in MATLAB in the function *ncfmargin* [11] and is used as fitness function or objective function of the Particle Swarm Optimization. The result is called fitness value and is used to determine the suitability of the chosen droop constants.

With the described method the Voltage Droop Control can be designed with maximized robustness, however, no account has been taken for electrical limits, yet. Consequently, only results are allowed where voltage, current and power limitations under any possible disturbance are maintained. The permissible voltage must be in a range of $\pm 10\,\%\,V_{\mathrm{DC,nom}}$. These electrical limitations are summarized as non linear constraints.

An optimization algorithm from [12] is used. It is based on the Particle Swarm Optimization, which is numerously published in literature, e.g. [13], [14], [15]. The entire flowchart is shown in Fig. 6.

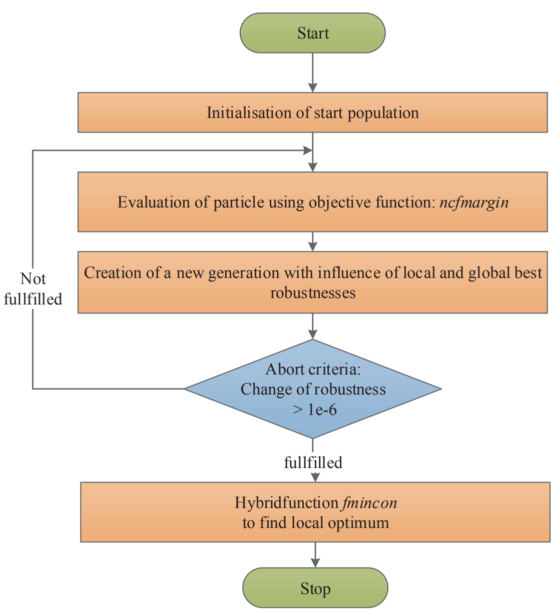

Fig. 6. Flow chart of the determination process of the droop constants with emphasis on robustness

V. Results

In order to discuss the results of the described methods, several simulations have been conducted and analysed. In the following the simulation of a radial parallel three terminal HVDC-system considering the droop constants of both presented methods for two operating points are compared.

In operating point one a power transmission from station B and C with 500 MW each to station A is established (Table I). At $t = 0.2\,\mathrm{s}$ the non-dominant station B trips and a power imbalance of +500 MW occurs. A station is called dominant if its absolute power is the highest compared to the absolute power of the other stations in the system.

TABLE I
Operating point one – DC-Voltage and Power

	Station A	Station B	Station C
$P_{\mathrm{DC,actual}}$ per pole in MW	978	-500	-500
V_{DC} in kV	411	420	420

In operating point two 995 MW are transmitted from station B to C. Station A doesn't take part in the transmission, but its Voltage Droop Control is active (Table II). After an outage of station B at $t = 0.2\,\mathrm{s}$ a power imbalance of 995 MW occurs.

TABLE II
Operating point two – DC-Voltage and Power

	Station A	Station B	Station C
$P_{\mathrm{DC,target}}$ per pole in MW	-0.08	994.92	-995
V_{DC} in kV	401.5	383	420

A. Method I - emphasis on electrical limits

Operating point one: Outage of station B: The droop constants of operating point 1 result from eq. (13) and are presented in Table III. After an outage of station B, which is working as rectifier, the voltage in the system decreases. At $t = 0.4\,\mathrm{s}$ the stationary value is reached.

TABLE III
Droop constants of operating point I with method I

K_{A} in $\frac{\mathrm{MW}}{\mathrm{kV}}$	K_{B} in $\frac{\mathrm{MW}}{\mathrm{kV}}$	K_{C} in $\frac{\mathrm{MW}}{\mathrm{kV}}$
23.03	11.77	11.77

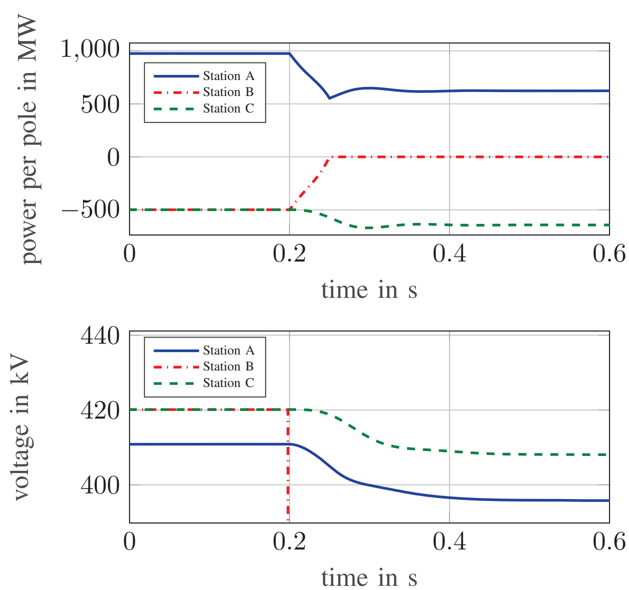

Fig. 7. Simulation of operating point I – Determination of the droop constants with method I

With eq. (3) and (1) the expected changes in power and voltage can be determined and are verified by the simulation results (Fig. 7). All electrical limits are maintained and the system is stable as well.

Operating point two: Outage of station B: As there is no or little power transmission of station A, a very small droop constant occurs (Table IV), which means that station A has no or little influence on balancing a power disturbance.

TABLE IV
DROOP CONSTANTS OF OPERATING POINT II WITH METHOD I

K_{A} in $\frac{\mathrm{MW}}{\mathrm{kV}}$	K_{B} in $\frac{\mathrm{MW}}{\mathrm{kV}}$	K_{C} in $\frac{\mathrm{MW}}{\mathrm{kV}}$
0.002	22.6	24.78

As seen in Fig. 8, the system is unstable and the system can't be operated with these droop constants. Due to the usage of the inverse of K as gain for the P-controller and a very small droop constant, the gain is very high. This leads to big disturbances in case of small deviations between actual and target value and the system is unstable.

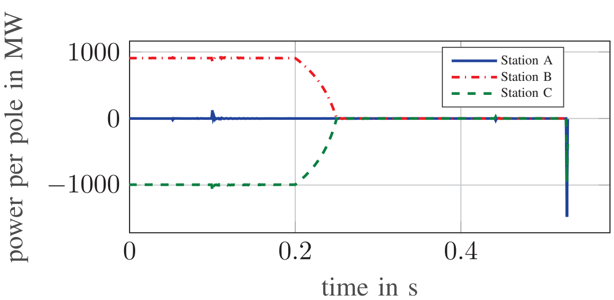

Fig. 8. Simulation of operating point II – Determination of the droop constants with method I

This method delivers good results for operating point one, as the system is stable and all electrical limits are maintained. However, for operating point two the system is unstable, due to a high gain of the P-controller. This must be prevented.

B. Method II

Operating point one: Outage of station B: Applying method II delivers droop constants with a robustness margin of 0.056 (Table V).

TABLE V
DROOP CONSTANTS OF OPERATING POINT I WITH PSO

K_{A} in $\frac{\mathrm{MW}}{\mathrm{kV}}$	K_{B} in $\frac{\mathrm{MW}}{\mathrm{kV}}$	K_{C} in $\frac{\mathrm{MW}}{\mathrm{kV}}$	Robustness R
3.96	14	9.25	0.056

After an outage of station B the power imbalance is distributed to obtain an equilibrium between the other stations. The calculation matches the simulation results (Fig. 9). The system is stable and optimized for robustness.

Operating point two: Outage of station B: For operating point two, the Particle Swarm Optimization delivers droop constants with a robustness of 0.054 starting from 2.24 $\frac{\mathrm{MW}}{\mathrm{kV}}$ to 42 $\frac{\mathrm{MW}}{\mathrm{kV}}$ (Table VI). The simulated system is, as well as in operating point I, stable and optimized for robustness. However,

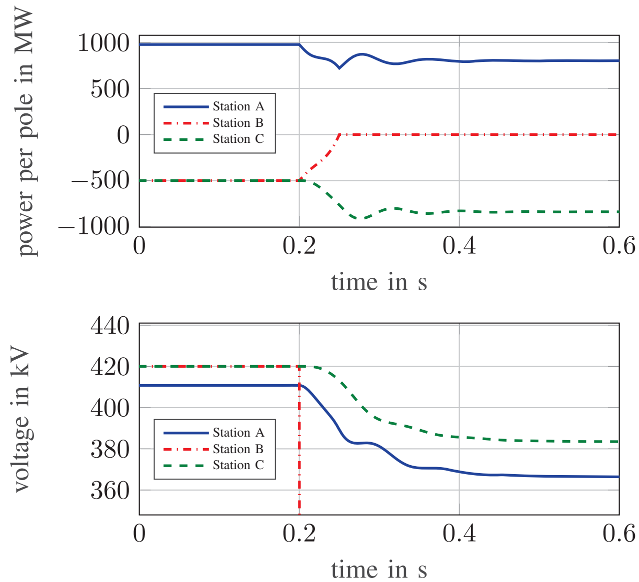

Fig. 9. Simulation of operating point I – Determination of the droop constants with method II

TABLE VI
DROOP CONSTANTS OF OPERATING POINT II WITH PSO

K_{A} in $\frac{\mathrm{MW}}{\mathrm{kV}}$	K_{B} in $\frac{\mathrm{MW}}{\mathrm{kV}}$	K_{C} in $\frac{\mathrm{MW}}{\mathrm{kV}}$	Robustness R
2.24	42	20.4	0.054

a transient oscillation can be seen between $0.2\,\mathrm{s} < t < 0.4\,\mathrm{s}$ (Fig. 10).

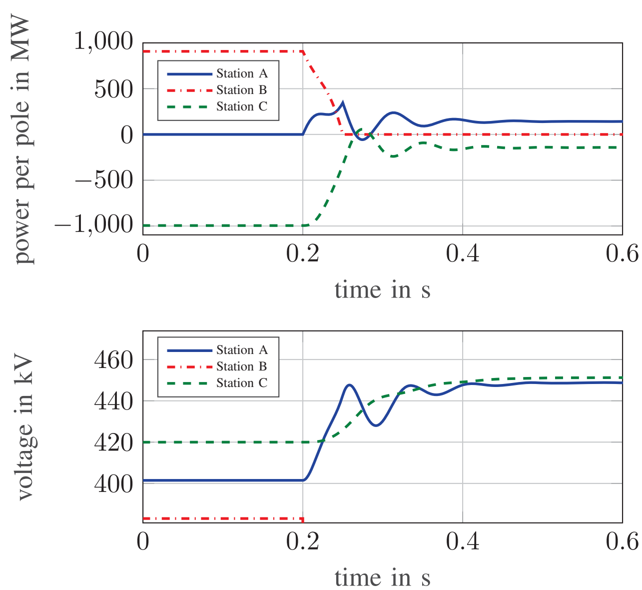

Fig. 10. Simulation of operating point II – Determination of the droop constants with method II

The Particle Swarm Optimization delivers applicable droop constants for all operating points. It optimizes the robustness and, thus, ensures stability. The computation of the Particle Swarm Optimization took several minutes on the used simulation PC. It is assumed, that the computation time on the target platform is in the same range. To overcome this issue, the droop constants are determined in advance and stored in a look-up-table, which can be accessed by the grid controller.

VI. Conclusion

In this paper, a concept for the determination of the droop constants for MT-VSC-HVDC-Systems is presented. Initially, a linear model of the system is introduced. Then, two methods are presented for the determination of the droop constants and, afterwards, their applicability is verified. This is performed by simulating and analysing an outage of a station.

TABLE VII
Summary of the results of the two methods

Method	Stability	Robustness	Electrical Limits	Computing Power
Power Limitation	–	–	+	++
Particle Swarm Optimization	+	++	+	–

Table VII gives an overview of the results of the examined methods. At first a method is introduced which calculates the droop constants with respect to electrical limits (Method I). It turns out, that the adapted method delivers applicable results for some operating points and the system is stable. Furthermore, all given electrical limits are maintained. However, in cases of small power transmission, an unstable system behaviour can occur. Thus, a determination with respect to robustness was analysed, which shall ensure stability. The Particle Swarm Optimization is used as optimization algorithm. This method delivers a maximum robustness margin of 0.0059 and applicable droop constants for all operating points.

References

[1] 50Hertz, Amprion, TenneT, TransnetBW - TSOs of Germany, *Grid development plan 2nd draft - Netzwentwicklungsplan Strom 2. Entwurf*, Berlin (Germany), 2014.

[2] R. Padiyar and N. Prabhu, "Modelling, control design and analysis of VSC based HVDC transmission systems," in *International Conference on Power System Technology*, Singapore (Singapore), Nov 2004.

[3] E. Prieto-Araujo, F. D. Bianchi *et al.*, "Methodology for Droop Control Dynamic Analysis of Multiterminal VSC-HVDC Grids for Offshore Wind Farms," *IEEE Transactions on Power Delivery*, vol. 26, pp. 2476–2485, 2011.

[4] F. Linke, A.-k. Marten, and D. Westermann, "Parametrierung einer kontinuierlichen DC-Spannungsregelcharakteristik für vermaschte HGÜ-Netze - Parameterization of a continouus DC-Voltage Droop Control for meshed HVDC grids," in *Power and Energy Student Summit (PESS)*, Dortmund (Germany), Jan 2015.

[5] F. Thams, J. A. Suul *et al.*, "Stability of DC voltage droop controllers in VSC HVDC systems," in *IEEE Eindhoven PowerTech*, Eindhoven (Netherlands), Jun 2015.

[6] M. Abdelwahed and E. El-Saadany, "Droop gains selection methodology for offshore multi-terminal HVDC networks," in *IEEE Electrical Power and Energy Conference (EPEC)*, Ottawa (Canada), Oct 2016.

[7] R. T. Pinto, S. F. Rodrigues *et al.*, "Comparison of direct voltage control methods of multi-terminal DC (MTDC) networks through modular dynamic models," in *14th European Conference on Power Electronics and Applications (EPE)*, Birmingham (UK), Aug 2011.

[8] K. Reinschke, *Linear automatic control and control theories - Lineare Regelungs- und Steuerungstheorie*. Berlin (Germany): Springer Publishing, 2014.

[9] T. Georgiou, "On the computation of the gap metric," *Systems & Control Letters*, vol. 11, pp. 253–257, 1988.

[10] S. Skogestad and I. Postlethwaite, *Multivariable feedback control: analysis and design*. New York (USA): John Wiley & Sons, 2005.

[11] Mathworks, *Dokumentation MATLAB R2017a – Optimization Toolbox*, 2017.

[12] S. Ebbesen, P. Kiwitz, and L. Guzzella, "A generic particle swarm optimization Matlab function," in *American Control Conference (ACC)*, Montreal (Canada), Jun 2012.

[13] G. Venter, J. Sobieszczanski-Sobieski *et al.*, "Particle Swarm Optimization," *AIAA Journal*, vol. 41, pp. 1583–1589, 2003.

[14] T. Zeugmann, P. Poupart *et al.*, "Particle Swarm Optimization," in *Encyclopedia of Machine Learning*, C. Sammut and G. I. Webb, Eds. Boston (USA): Springer Publishing, 2011, vol. 33, pp. 760–766.

[15] R. Poli, J. Kennedy, and T. Blackwell, *Particle swarm optimization Volume 1, Issue 1*. Berlin (Germany): Springer Publishing, 2007.

Biographies

Michael Endres received his B.Eng. in electrical engineering from the Technical University of Nuremberg, Germany, in 2014 and his M.Sc. from Friedrich-Alexander University Erlangen-Nuremberg in 2017. From 2010 through 2017 he was working at Siemens Energy Management in the field of HVDC and SVC. His research interests lie in the field of HVDC and power transmission

Christoph Hahn (M'2012) received his Dipl.-Ing. degree from the University of Erlangen-Nuremberg, Germany, in 2011. Currently he is research associate and working towards a Ph.D. at the Institute of Electrical Energy Systems at the University of Erlangen-Nuremberg, Germany. His research interests lie in the field of HVDC modeling and control.

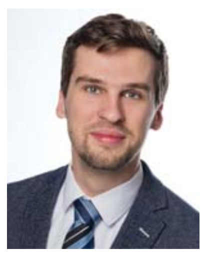

Jens Dietrich received his B.Sc. and M.Sc. in Electrical Engineering from RWTH Aachen University in 2013 and 2016 respectively. Currently he is employed at Siemens AG, Germany as a system engineer for control and protection of HVDC systems. His research interests lie in the modeling and control of HVDC systems as well as software architectures for large control systems.

Yannick Fotsing received his Masters degree in control system from University of Kaiserslautern, Germany in 2011. From 2011 through 2015, he worked at Siemens Industry, Germany on the modeling and control of power-electronic converters. Since 2016, he is with Siemens Energy Management, Germany, where he is in charge of the development of a Grid Controller for MT-HVDC systems.

Matthias Luther (M'2011) studied electrical engineering and received his Ph.D. at the Technical University of Brunswig, Germany in 1992. From 1993 he held different functions and management positions in the electricity industry at PreussenElektra, E.ON Netz and TenneT TSO. Since 2011 he is professor and is head of the Institute of Electrical Energy Systems at the University of Erlangen-Nuremberg, Germany.